Received: 25 November 2020 | Accepted: 8 January 2021

DOI: 10.1111/gcb.15544

Global Change Biology WILEY

PRIMARY RESEARCH ARTICLE

Short- and long-term carbon emissions from oil palm plantations converted from logged tropical peat swamp forest

Jon McCalmont[1] | Lip Khoon Kho[2] | Yit Arn Teh[3] | Kennedy Lewis[1] | Melanie Chocholek[4] | Elisa Rumpang[2] | Timothy Hill[1]

[1]College of Life and Environmental Science, University of Exeter, Exeter, UK

[2]Tropical Peat Research Institute, Biological Research Division, Malaysian Palm Oil Board, Kajang, Selangor, Malaysia

[3]School of Natural and Environmental Science, Newcastle University, Newcastle-upon-Tyne, UK

[4]Department of Earth and Environmental Science, University of St. Andrews, St. Andrews, UK

Correspondence
Jon McCalmont, College of Life and Environmental Science, University of Exeter, Streatham Campus, Rennes Drive, Exeter EX4 4RJ, UK.

Funding information
Malaysian Palm Oil Board

Abstract

Need for regional economic development and global demand for agro-industrial commodities have resulted in large-scale conversion of forested landscapes to industrial agriculture across South East Asia. However, net emissions of CO_2 from tropical peatland conversions may be significant and remain poorly quantified, resulting in controversy around the magnitude of carbon release following conversion. Here we present long-term, whole ecosystem monitoring of carbon exchange from two oil palm plantations on converted tropical peat swamp forest. Our sites compare a newly converted oil palm plantation (OPnew) to a mature oil palm plantation (OPmature) and combine them in the context of existing emission factors. Mean annual net emission (NEE) of CO_2 measured at OPnew during the conversion period (137.8 Mg CO_2 ha^{-1} $year^{-1}$) was an order of magnitude lower during the measurement period at OPmature (17.5 Mg CO_2 ha^{-1} $year^{-1}$). However, mean water table depth (WTD) was shallower (0.26 m) than a typical drainage target of 0.6 m suggesting our emissions may be a conservative estimate for mature plantations, mean WTD at OPnew was more typical at 0.54 m. Reductions in net emissions were primarily driven by increasing biomass accumulation into highly productive palms. Further analysis suggested annual peat carbon losses of 24.9 Mg CO_2-C ha^{-1} $year^{-1}$ over the first 6 years, lower than previous estimates for this early period from subsidence studies, losses reduced to 12.8 Mg CO_2-C ha^{-1} $year^{-1}$ in the later, mature phase. Despite reductions in NEE and carbon loss over time, the system remained a large net source of carbon to the atmosphere after 12 years with the remaining 8 years of a typical plantation's rotation unlikely to recoup losses. These results emphasize the need for effective protection of tropical peatlands globally and strengthening of legislative enforcement where moratoria on peatland conversion already exist.

KEYWORDS
carbon emission, carbon stocks, ecosystem carbon exchange, eddy covariance, land-use change, oil palm plantation, peatland drainage, tropical peatland conversion

1 | INTRODUCTION

The need for economic development across South East Asia, and global demand for agro-industrial commodities such as palm oil, rubber and pulp wood have driven the expansion of industrial-scale agriculture and associated land-use change in recent decades. Agricultural crop production now covers 122 million hectares in the region (Kenney-Lazar & Ishikawa, 2019), around a quarter of the total land area.

In Malaysia and Indonesia alone, oil palm plantations now cover an estimated 23 million hectares (Cheng et al., 2018; Gaveau et al., 2018; Miettinen et al., 2017). A significant proportion of this conversion has occurred recently on tropical peatlands; between 1990 and 2015, some 7.8 million hectares of these wetland peat swamp forests (PSFs) were converted through forest clearance and land drainage (Miettinen et al., 2016). The economic contribution of expanding oil palm production, particularly in rural areas (Qaim et al., 2020), has come at a, yet to be fully determined, cost to the local environment and the global carbon balance.

Conversion of tropical forests, and particularly PSFs, results in carbon emission (Cook et al., 2018; Couwenberg et al., 2009; Manning et al., 2019; Miettinen et al., 2017; Wijedasa et al., 2018), biomass loss (Kho & Jepsen, 2015), changes in carbon cycling dynamics (Swails et al., 2017) and the disturbance of previously stable soil carbon pools (Cheng, 2009; Kuzyakov, 2010). The majority of studies to date have employed subsidence and/or soil surface respiration measurements to estimate soil organic carbon (SOC) losses and estimates vary greatly, ranging (as CO_2-equivalent) from 20 to 100 Mg CO_2 ha^{-1} $year^{-1}$ (e.g. Cooper et al., 2020; Couwenberg & Hooijer, 2013; Dariah et al., 2014; Hergoualc'h et al., 2017; Hooijer et al., 2012; Ishikura et al., 2018; Manning et al., 2019; Melling et al., 2005; Wösten et al., 1997). While different experimental techniques and/or sampling designs may be influencing this variability, site-specific factors are thought to strongly contribute to the wide range of observed SOC losses.

Measurements from soil surface chambers and subsidence focus on SOC losses which is often advantageous, but these measurements do not allow direct monitoring of the net CO_2 change in the atmospheric carbon pool as they cannot concurrently capture photosynthetic carbon uptake and above-ground sources of CO_2. In this regard, the eddy covariance (EC) technique (Baldocchi, 2003) provides distinct advantages: EC measures the net ecosystem exchange (NEE) of carbon, capturing both emission and uptake, and spatially integrates over complex intra-site sources, such as drainage ditch peat extraction and autotrophic respiration from plant biomass. EC has previously been employed in peatland forests in the region; Hirano et al. (2012) used it to investigate the impact of large-scale anthropogenic disturbance on the carbon balance of tropical PSF in Indonesian Borneo, concluding that PSF were all now likely to be sources of atmospheric carbon (in the range of 7–18 Mg CO_2 ha^{-1} $year^{-1}$). A conclusion supported by another, very recent, EC study in logged PSF that showed a mean net emission of CO_2 over 4 years at 15.4 Mg CO_2 ha^{-1} $year^{-1}$ (Tang et al., 2020). However, the logistical and financial costs associated with EC have, to date, limited its deployment (Hill et al., 2017) and more studies are needed in tropical peatlands.

Only very recently have studies using EC started to report net carbon flux from oil palm plantations (Meijide et al., 2020), with only one monitoring oil palm cultivation on tropical peat (Kiew et al., 2020). The Kiew et al. (2020) study monitored a mature oil palm plantation on peatland in Sarawak, Malaysia and reported a mean annual net emission of 36.4 Mg CO_2 ha^{-1} $year^{-1}$, three times the Meijide et al. (2020) estimate for oil palm on mineral soils and double the emissions seen in even the most disturbed PSF reported in Hirano et al. (2012). Kiew et al. (2020) echoed Meijide et al. (2020) in calling for more EC studies on peatland plantations, particularly in the early years of conversion where net emissions are expected to be at their highest but are, as yet, unreported. The implications of this lack of EC monitoring of different age classes of peatland oil palm is significant; Meijide et al. (2020) state they were unable to perform a full carbon life cycle assessment (LCA) as a result, despite the need for better quantification being highlighted in earlier LCA studies of palm oil production (Mattsson et al., 2000; Schmidt, 2015).

In the absence of field studies of oil palm peatland conversions across the entire cultivation lifetime, emission factors determined for tropical forest conversion to agriculture on peatland have so far had to rely on very limited data. In deriving their Tier 1 emission factor of 40 Mg CO_2 ha^{-1} $year^{-1}$ for conversions to oil palm on drained peatland, the IPCC list only eight direct studies, of which six were soil flux chamber studies and two were based on subsidence measurements. No ecosystem-level monitoring of carbon flux was available to be included in the assessment. The IPCC (Hiraishi et al., 2014) stated that emissions during the early years of plantation establishment are expected to be significantly higher than their emission factor but were not included due to this lack of available data.

The absence of directly measured net carbon flux from peatland conversions to industrial plantation led to controversy around the GWP impacts of conversion (Wijedasa et al., 2017). Reviewers for an Environmental Protection Agency (EPA) report into peatland emission factors for oil palm (EPA, 2014) were split over the importance of these early year emissions; debating the evidence of Hooijer et al. (2012) who had reported that very rapid subsidence recorded in the first 5 years of conversion was the result of large CO_2 emissions. There was a suggestion that compaction may be contributing more to this large initial subsidence than the Hooijer et al. (2012) study might suggest, and that there was not enough scientific evidence to the contrary.

Despite their limitations, current emission factors continue to play a crucial role in informing national and international policy. The industry standard Round Table on Sustainable Palm Oil, the world's largest certification initiative for palm oil (Qaim et al., 2020), rely on two synthesis studies, Hooijer et al. (2010, 2012), as the key components in their assessment of the peat carbon impact of peatland conversion. The figure of CO_2 (Mg CO_2 ha^{-1} $year^{-1}$) emissions being 91 times water table depth (WTD; m) from Hooijer et al. (2010) is the default value in their current GHG calculator (https://rspo.org/certi

fication/palmghg/palm-ghg-calculator) which underpins estimates of peat decomposition in their certification scheme (https://rspo.org/certification). This coefficient of 91 was derived from a linear fit (with a fixed intercept of zero) to just eight data points collated from five studies, yet plays an important role in modelling the global carbon budget (Friedlingstein et al., 2019; Houghton & Nassikas, 2017; Le Quéré et al., 2018).

In this study, we begin to address this important knowledge gap by contributing data collected by EC at two adjacent oil palm plantations established on tropical peatlands in South East Asia. One site captures a period following the initial conversion from PSF and another captures the mature phase. We present annual net ecosystem CO_2 fluxes from individual measurement years at both sites and partition them into photosynthetic uptake and whole ecosystem respiration. We then combine both data sets into a single chronosequence over a 151-month period and use a mass balance approach (incorporating estimates of biomass accumulation and forest residue decomposition) to calculate changes in soil carbon stocks. We present emission factors both for individual years and across relevant time periods (e.g. years 1–6, as highlighted by the IPCC). Finally, we investigate the relationship between soil water drainage and carbon loss in the context of previous emission coefficients and consider the potential impact of changes in plantation drainage targets.

2 | METHODS

2.1 | Site location and description

The two study sites were individual blocks of commercially managed oil palm plantation situated within the Sabaju (OPnew: 3°9.615′N, 113°25.163′E) and Sebungan (OPmature: 3°9.965′N, 113°21.198′E) plantation estates in Sarawak, northern Malaysian Borneo. Climate is tropical equatorial with stable air temperatures (mean 26°C) and high humidity and rainfall, typically ~3000 mm $year^{-1}$. The sites are located 7.3 km from each other and represent typical oil palm plantation established on deep peat (up to 8 m) in the region. Both sites were established into previously logged PSF cleared and drained by cutting a regular network of drainage channels prior to palm establishment (see Cook et al., 2018 for a more detailed description of the plantation estates). The previously degraded forest at OPnew was cleared (without burning) at the beginning of 2016 with forest biomass cut and compacted on site and drainage channels cut into the peat. Establishment of oil palm (~160 plants ha^{-1}) was completed by the end of April 2016 and followed commercial practice throughout, no harvest was taken from the immature palms at OPnew during the study period. OPmature was established in July 2007 with fruit bunch harvesting (fresh fruit bunch [FFB]) beginning from month 32. EC monitoring at OPnew begins 4 months after forest clearance and continues for 41 months while at OPmature it begins 10 years after conversion and continues for 33 months.

2.2 | Instrumentation

Eddy covariance was carried out at both sites using identical instrumentation with the only significant difference being that profile measurements, for canopy storage of CO_2 and energy, were from three heights on a 20-m tower for the taller palms at OPmature compared to two on a 6-m tower at OPnew. LI-COR closed path systems (LI-7200/7550; LI-COR Environmental coupled to R3-50 Sonic Anemometer; Gill Instruments Ltd.) were used at both sites, with sensors sited at the top of each tower. For OPmature this resulted in a measurement height (above-ground) of 20.19 m, approximately 12 m above an 8 m canopy; for OPnew, sensors were at 6.06 m above a canopy that reached 2.6 m by the end of the study period. Prior to canopy development at OPnew topography was dominated by forest destruction residues compacted into rows of approximately 2 m in height which gave a typical measurement height above canopy of around 4 m. Canopy profile CO_2 and energy storage was measured using CO_2 diffusion sensors coupled with air and relative humidity sensors (GMP343 and HMP155A; Vaisala Corporation). For OPmature these were placed at 1, 6 and 18 m above-ground, for OPnew this was at 1 and 6 m. Energy balance was monitored at two locations for each site using heat flux plates (HFP01SC; Hukseflux Thermal Sensors) at 0.08 m soil depth coupled to soil moisture/temperature sensors (Steven's Hydraprobe; Stevens Water Monitoring Inc.) at 0.04 m. WTD was monitored within 0.05-m-diameter porous plastic pipe inserted to a depth of 2.5 m (PX709GW submersible pressure transducer; Omega Engineering Inc.). Precipitation was measured at the top of each tower using a tipping bucket gauge (TR-525M; Texas Electronics). EC data were collected at 10 Hz and written to an industrial-grade USB drive within the LI-7550, meteorological data at 1-minute intervals stored to Xlite 9210 dataloggers (Sutron Corporation).

2.3 | Eddy covariance data processing

2.3.1 | Flux calculations

Raw flux data (10 Hz) were initially processed into 30-min average CO_2 flux rates (μmol CO_2 m^{-2} s^{-1}) using EddyPro software (v6.2.2 LI-COR Environmental) before being storage corrected, gap-filled and further summed into mass integrations of NEE over time (e.g. Mg CO_2-C ha^{-1} $month^{-1}$). Data handling, quality control and analyses were carried out using R (v3.5.1, R Core Team, 2018; R Foundation for Statistical Computing).

Statistical outliers (spikes) in the 10 Hz data were detected following Vickers and Mahrt (1997); vertical wind speed measurements were only accepted at <5 SDs (σ) from the 30-min mean, other variables at 3.5σ; 30-min periods containing spikes at greater than 1% were flagged as poor quality. Time lags, discrepancies between precise sampling times at the anemometer and gas analyser, are compensated for using site-specific covariance maximization derived from data collected at the site. Detrending of turbulence fluctuations over each

30 min was through block averaging. Co-ordinate rotation, to accommodate imperfect alignment to the horizontal wind vector, was carried out through the planar fit method of Wilczak et al. (2001) using site-derived parameters. Co-spectral analysis and correction of low- and high-pass filtering effects were carried out following Moncrieff et al. (1997, 2004). Spatial estimation of the areal source of sensor data capture (footprint assessment) followed Kljun et al. (2004) or Kormann and Meixner (2001), where turbulent friction was <0.2 m s^{-1}. CO_2 storage below the sensor height, which is not captured in turbulent eddy transfer through the EC sensor pathways, was accounted for through profile monitoring of CO_2 concentrations between the ground and sensor heights as outlined in Baldocchi et al. (2001): time-stamped changes in absolute CO_2 concentration are captured by profile sensors and converted to volumetric ratios using the ideal gas law. These are then added to the corresponding flux measurements captured by EC at the half-hour time step.

2.3.2 | Quality control flagging

Initial quality control flagging of each 30-minute flux average (statistical testing of the 10 Hz data) followed the Carbo-Europe standard 0-1-2 system of Foken et al. (2004). Zero being the highest quality, values flagged at 2 were automatically discounted from further processing. Data spikes in the half-hourly processed CO_2 data were identified and removed following Papale et al. (2006) using the suggested median deviation threshold (z value) of 4. Absolute thresholds for sensible heat (H) were set between −200 and 350 W m^{-2} and for latent energy (LE) at −50 to 500 W m^{-2}.

2.3.3 | Study site area (measurement fetch and footprint)

The available study area which satisfied EC assumptions of homogeneity and representation of the area of interest (fetch) covered 41.7 ha at OPnew and 907 ha at OPmature. A combination of Google Earth (GE v7.3.2.5776, Imagery date 24/03/2016) and ARCGIS (ArcMap 10.5.1; ESRI) was used in conjunction with the output from the footprint model to filter out any measurement periods where data collection extended beyond the ideal fetch. Taking the sensor tower location as a datum point, distances to the edge of the fetch boundary were measured at 10° increments. Half-hourly output from the footprint model (percentage data contribution to total, distance to peak contribution and wind vector) was compared to these boundaries within 10° bins (total of 36) and considered acceptable where 70% of the information collected in each half-hour was sourced within the fetch boundary.

2.3.4 | Energy balance

Energy balance closure (EBC) was investigated using an ordinary least square (OLS) regression at the half-hour time step between turbulent heat flux (LE plus H) and available energy (net radiation plus soil heat flux). EBC was considered as the slope of the resulting OLS fit. Energy storage in relevant pools (canopy air space and soil volume) was calculated using specific heat capacity and moisture fluctuations. Energy lost to photosynthetic utilization was calculated following Masseroni et al. (2014). The ratio between turbulent heat flux and available energy over the entire study period is presented as the energy balance ratio following Wilson et al. (2002).

2.3.5 | Gapfilling and flux partitioning

Gapfilling of data rejected through quality control and partitioning of NEE into photosynthetic uptake (gross primary productivity [GPP]) and ecosystem respiration (R_{eco}) was carried out using the ReddyProc package (Wutzler et al., 2018) within R. For gapfilling, this package utilizes the mean diurnal separation (MDS) approach of Falge et al. (2001) with flux partitioning carried out using the light response curve method of Lasslop et al. (2010) to estimate daytime GPP, the sum of NEE and GPP being R_{eco}. Night-time fluxes (below a global radiation (R_g) threshold of 20 W m^{-2}) are assumed solely R_{eco} (Reichstein et al., 2005). Underestimation of fluxes during periods of insufficient turbulence was avoided by removing data recorded below site-derived friction velocity thresholds (u^* filtering) during the gap-filling process (Reichstein et al., 2005). Uncertainties in the half-hour fluxes are calculated, for gapfilled values, as the standard error of the mean (SEM) of the values used to fill gaps. For retained original data these are artificially marked as gaps and again the standard error is calculated for the mean of values that would have been used to fill them. Standard errors are then propagated through cumulative sums.

2.3.6 | Chronosequence data series

Data collection from OPnew starts from the beginning of September 2016 and runs to the end of January 2020, this represents months 5–45 in the plantation's life cycle. For OPmature, data start from May 2017 and again run to January 2020, capturing months 119–151 of that plantation's life cycle.

The first 4 months of data immediately following the conversion of PSF at OPnew were not collected due to the sensor installations not yet being in place. An estimation of these values has been made through modelling backwards at a monthly time step from the first data available. For GPP, an assumption is made that this would be zero immediately following conversion (dead forest residues and bare soil), therefore linear interpolation was carried out from a start point of zero at the beginning of May 2016 to the beginning of September 2016 (the first complete month's data). For R_{eco}, a linear trend line was fitted to the existing R_{eco} monthly data set and extended back over these first 4 months.

Trends in fluxes (GPP, R_{eco} and NEE) over the measurement period at each site are indicated by the slope of a linear model fitted against

time, with significance accepted at $p < 0.05$. Estimation of annual means within specific periods is calculated by multiplying the mean monthly values for that period by 12. A complete chronosequence of NEE, from months 1–151 was established using exponential interpolation (Stineman, 1980) between the OPnew and OPmature data sets at a monthly time step. This interpolation was also applied to months 141–146 (April 2019–August 2019) at OPmature, where data were excluded due to sensor malfunction resulting in a gap too large for the MDS gap-filling routine.

2.4 | Calculation of net primary productivity

2.4.1 | Live standing biomass

Net primary productivity (NPP) is the sum of photosynthetic carbon sequestered into biomass pools on site during any given period. For live palm biomass carbon stocks, data were interpolated at a monthly time step between biomass, and associated carbon concentration, for age classes 3, 8 and 12 years, measured from destructive sampling from appropriately aged planting blocks at the Sabaju (age classes 3 and 8 years) and Sebungan plantations (age class 12 years) in 2019 and presented in Lewis et al. (2020). Individual palm component carbon stocks are summed to total palm biomass carbon using Equation (1). Root biomass was not directly sampled in Lewis et al. (2020) so has been assumed at 16% of total standing biomass following Khalid et al. (1999). This resulted in a timeseries of biomass carbon stocks across months 1–144; differences between values at the beginning and end of periods correlated with the EC flux measurements give NPP for that period (Equation 2).

$$\begin{aligned}\text{Carbon}_{\text{biomass}} = &\text{Carbon}_{\text{roots}} + \text{Carbon}_{\text{trunks}} + \text{Carbon}_{\text{frondbases}} + \text{Carbon}_{\text{fronds}} \\ &+ \text{Carbon}_{\text{FFB}} + \text{Carbon}_{\text{spears}} + \text{Carbon}_{\text{cabbage}} + \text{Carbon}_{\text{residual}},\end{aligned} \quad (1)$$

where all components' dry mass multiplied by fraction of carbon content (see Table S.1.2 for full details)

$$\text{NPP}_{\text{period}} = \text{Carbon}_{\text{biomass}(t)} - \text{Carbon}_{\text{biomass}(t-\text{period})}, \quad (2)$$

where NPP denotes the net primary productivity (carbon sequestered into vegetative biomass, Mg CO_2-C ha^{-1}) and t denotes time (period [months])

2.4.2 | Fresh fruit bunch harvest offtake

Harvest offtake, as FFB, was provided by the site managers for the OPmature planting block specifically within the Sebungan plantation at a monthly time step from the date of first harvest in month 32 to month 144. For months 0–31, linear interpolation was used to complete the monthly timeseries from zero to first harvest. For sequestration calculations, all FFB is considered to remain within the system (see Section 4), therefore total NPP of FFB for any given period is the cumulative sum of all harvest offtake during that period.

2.4.3 | Pruned frond biomass

At each harvest, a number of fronds are cut to facilitate access to FFB and left in piles to decompose on site. While uptake of carbon into these fronds during growth, and return to atmosphere through decomposition, will be captured by EC in NEE, the carbon stored within the ecosystem in the total frond pile biomass at any given time needs to be accounted for in NPP. An estimate for this was derived from monthly interpolation between the numbers of frond bases (remnants of removed fronds) present on the palms at the 3-, 8- and 12-year time points. While multiplying these by a mean frond mass (for each age class of frond, similarly interpolated) gives an estimate of frond mass pruned in each month, account needs to be taken of the decomposition of each monthly addition to the pruned frond pile over the remaining study period. This was carried out by applying an exponential decay function, Equation (3) (Moradi et al., 2014; Olson, 1963) to each monthly pruned frond mass and continuing to the end of the chronosequence, then summing across the remaining biomass from all previous prunings to a total pruned frond biomass pool per hectare for each month. The decomposition rate constant (fractional mass loss per month [k]) for frond biomass was set at 0.15, calculated from empirical measurements by Moradi et al. (2014).

$$\text{mass}_t = \text{mass}_{t-1} \cdot \exp^{(-kt)}, \quad (3)$$

where t denotes time (month) and k denotes decomposition rate constant (fractional mass loss per month).

2.5 | Calculation of forest debris decomposition

The contribution to ecosystem respiration (R_{eco}) from the decomposition of the previous forest biomass (R_{fr}) that was cut and compacted on site prior to establishment of oil palm needs to be considered in the overall carbon budget as these emissions will be a significant contribution to the net flux captured by EC. Starting biomass and decomposition rate were not measured directly on site, so literature estimates have been used. As with the frond pile biomass, the decay rate for forest coarse woody debris (CWD) decomposition is calculated using Equation (3) at a monthly time step, but in this case just considers a single biomass addition at the beginning of the conversion. Kho and Jepsen (2015) estimated 58.7 ± 10.7 Mg C ha^{-1} for logged PSF (as at OPnew); using their dry stem biomass carbon content of 47.4%, we derive forest biomass at clearance of 123.8 ± 22.6 Mg DM ha^{-1}. Only one paper was found that monitored CWD decay under tropical peatland conditions in the same region (Law et al., 2019), who were working in Sabah, Malaysian Borneo under very similar climatic conditions to this present study. That study reported that after 12 months there had been a mean loss of

25.6% of the starting biomass. From this we calculated a rate constant (k) at 0.02464 for decomposition of forest CWD at a monthly time step which would result in the correct biomass loss by month 12.

2.6 | Changes in SOC

Changes in SOC (ΔSOC) during specific periods were calculated as the difference between GPP and R_{eco}, taking account of sequestration of GPP into biomass stocks (NPP) and contribution of R_{fr} to R_{eco}. Following production of a complete monthly timeseries of NPP and R_{fr}, as described above, periods corresponding to direct measurements of NEE (partitioned into GPP and R_{eco}) were used as parameters in Equation (4) to estimate peat carbon loss for the study period months at OPnew and OPmature. For annual carbon emission factors over the entire 151-month chronosequence of NEE, and for specified periods, Equation (4) is modified using Equation (5) (see Equation S.2.1) and uses parameters derived by taking mean monthly values within selected time periods and multiplying by 12. Emission factors were calculated for years 0–6 (establishment), 6–12 (mature) and across the entire period. Additional exports of carbon (ε), such as drainage losses of dissolved and particulate organic carbon or methane emissions (CH_4), are not captured in our EC results and are therefore not accounted for in these calculations; however, their potential magnitude is considered in the discussion section below.

$$\Delta SOC = \frac{(GPP - (R_{eco} + NPP) + R_{fr}) - \varepsilon}{t}, \quad (4)$$

where ΔSOC is the change in soil organic carbon (Mg CO_2-C ha^{-1}), GPP is the gross primary productivity (photosynthetic uptake of carbon, Mg CO_2-C ha^{-1}), R_{eco} is the Ecosystem respiration (Mg CO_2-C ha^{-1}), NPP is the net primary productivity (carbon sequestered into biomass, Mg CO_2-C ha^{-1}), R_{fr} is the respiration contribution from decomposition of forest residue (Mg CO_2-C ha^{-1}), ε denotes the unaccounted factors (e.g. export as dissolved organic carbon, carbon content of emitted CH_4, etc., Mg CO_2-C ha^{-1}) and t denotes the time (year)

$$NEE = R_{eco} - GPP, \quad (5)$$

where NEE is the net ecosystem exchange of carbon (Mg CO_2-C ha^{-1})

2.7 | Relationship between peat carbon loss and WTD

The relationship between our estimate of SOC emission (as CO_2) and WTD was considered in two separate analyses. Firstly, at an annual time step in the context of the Hooijer et al. (2010) analysis, by the recreation of their original linear regression (from data provided in Hooijer et al. (2006)) and subsequent inclusion of annual ΔSOC from OPnew and OPmature. Secondly, taking advantage of our high-frequency respiration data (at the half-hour time step) at OPnew, we fit a non-linear second-order polynomial curve to nighttime NEE, assumed to be entirely respiration, and WTD following detrending of the data series and binning of R_{eco} into 0.01 m increments of WTD. Only original measured data (not gapfilled) were used and selected at the highest quality (qc flagged at zero; Foken et al., 2004). The output of the model fit was then used to predict respiration rates for 0.1 m WTD increments between 0 and 0.8 m below the soil surface (the measured WTD range at OPnew within the study period).

3 | RESULTS

See Supporting Information for full details of EC data capture and retention following quality control. Values ± given throughout these results indicate the standard error of the mean (SEM)

3.1 | Climate data

As expected in equatorial, tropical climate rainfall was high and temperatures were relatively stable over time with only a minimal seasonal component (Figure 1). Rainfall averaged 2856 ± 96 mm $year^{-1}$ across the two sites, and had a mean temperature of 26.9 ± 0.03°C. The exposed soils at OPnew were on average 2°C warmer than at OPmature, with a mean soil temperature in the upper 0.04 m of 30.3 ± 0.03°C compared with 28.3 ± 0.03°C under the canopy at OPmature. The mean WTD was 0.26 ± 0.04 m at OPmature and 0.54 ± 0.05 m at OPnew.

3.2 | Measured carbon flux (as CO_2)

3.2.1 | Ecosystem respiration

A small, but statistically significant, difference was seen between mean monthly R_{eco} at the two sites (Welch two-sample t test, t = 7.2, df = 47.4, p < 0.0001). OPnew was higher at 17.6 ± 0.4 Mg CO_2 ha^{-1} $month^{-1}$ (± SEM of monthly totals) compared to OPmature 14.2 ± 0.4 Mg CO_2 ha^{-1} $month^{-1}$. For OPnew, there was no significant change in monthly R_{eco} over the monitoring period (F = 0.6, df = 39, p = 0.4); in contrast, at OPmature there was a slight, but significant, decline in R_{eco} over time, reducing by 0.11 Mg CO_2 ha^{-1} $month^{-1}$ (f = 6.35, df = 25, p = 0.02).

3.2.2 | Photosynthetic uptake

Monthly GPP at OPnew showed a significant increase over the study period (f = 194.7, df = 39, p < 0.0001); from 1.1 Mg CO_2 ha^{-1} $month^{-1}$ in September 2016 (4 months after

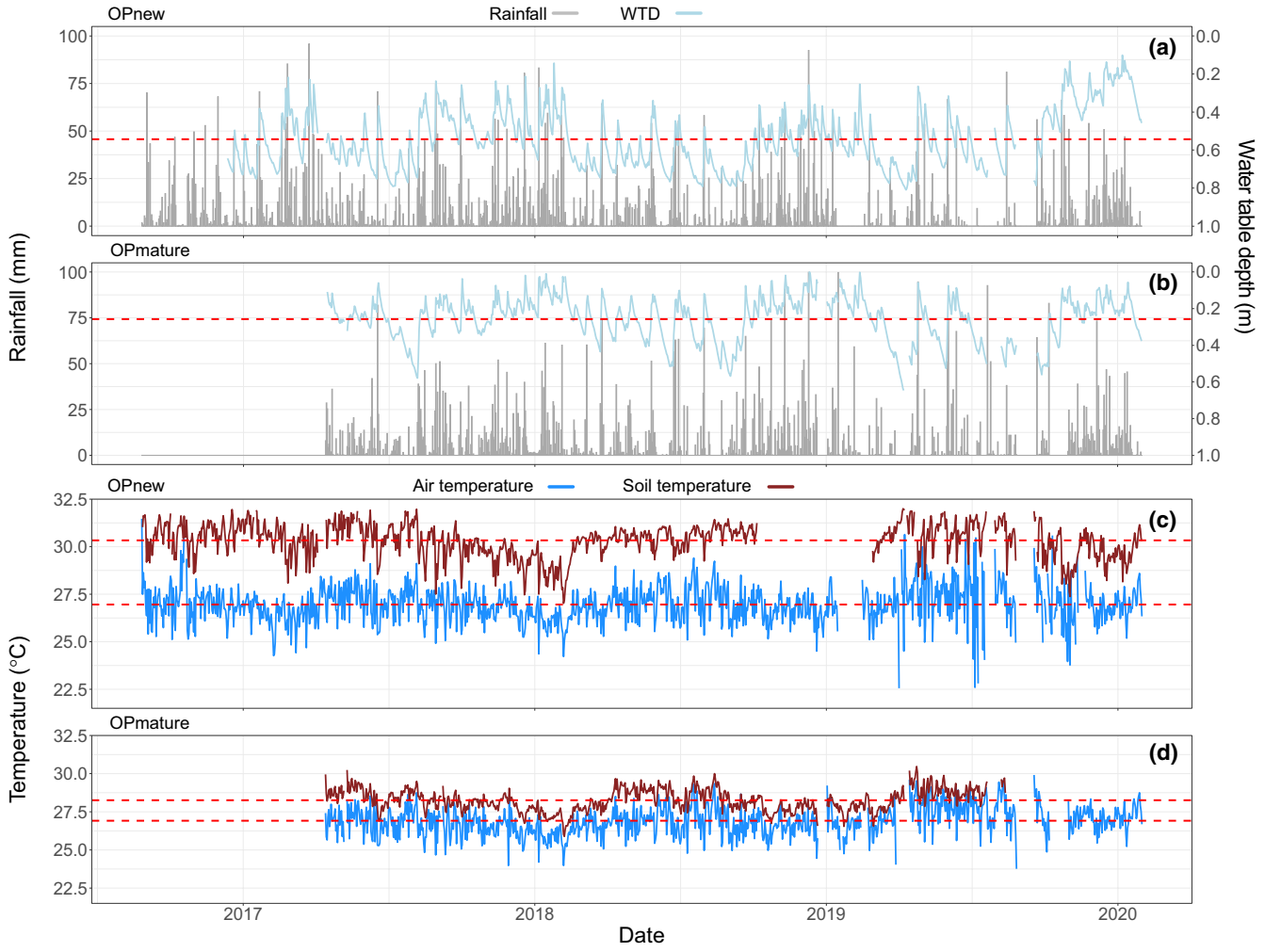

FIGURE 1 Daily climate data from OPnew and OPmature. Plots (a) and (b) show rainfall (left *Y* axis) and water table depth (right *Y* axis) for each site with mean water table depth (WTD) indicated by a dashed red line. Plots (c) and (d) show air and soil temperature at each site, again with dashed red lines indicating the mean for each parameter over the study period

FIGURE 2 Monthly total CO_2 flux for OPnew and OPmature partitioned into gross photosynthetic uptake (GPP) and ecosystem respiration (R_{eco}). *X* axis labels indicate sampling date, inset year labels indicate which growing year (post-plantation establishment) each monitoring period overlaps

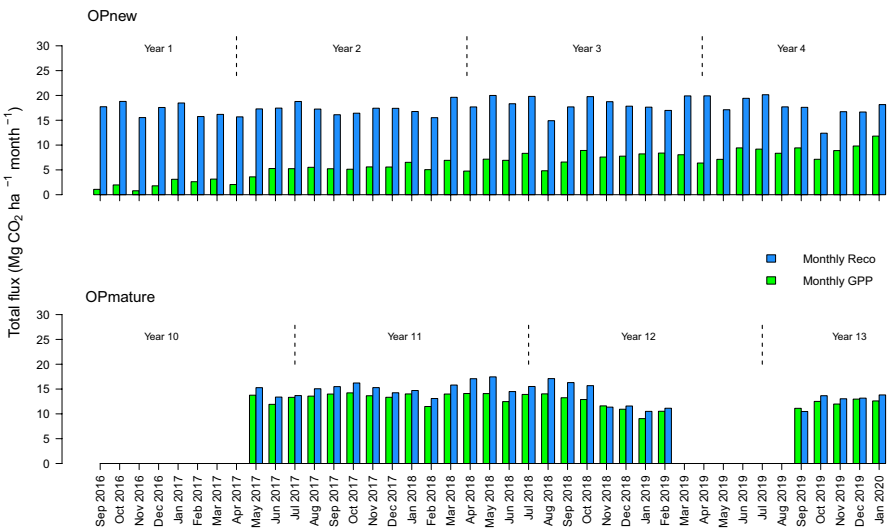

conversion) it increased by 0.18 Mg CO_2 ha^{-1} $month^{-1}$. GPP at OPmature also changed over time, but in this case showed a small, but significant, reduction in uptake; declining over the study period by 0.07 Mg CO_2 ha^{-1} $month^{-1}$ (f = 6.35, df = 25, p < 0.05). Mean monthly GPP was 6.2 ± 0.4 Mg CO_2 ha^{-1} $month^{-1}$ at OPnew and 12.8 ± 0.2 Mg CO_2 ha^{-1} $month^{-1}$ at OPmature (Figure 2).

3.2.3 | Net ecosystem exchange

Both sites were cumulative net sources of carbon to the atmosphere, with a mean annual NEE calculated over the entire study period of 137.8 ± 4.9 Mg CO_2 ha^{-1} $year^{-1}$ at OPnew and 17.5 ± 2.1 Mg CO_2 ha^{-1} $year^{-1}$ at OPmature. Only two monthly totals of NEE showed a net uptake, and both were at OPmature: November 2018 at −0.3 Mg CO_2 ha^{-1} $month^{-1}$ and September 2019 at −0.6 Mg CO_2 ha^{-1} $month^{-1}$. NEE decreased significantly during the study period at OPnew (f = 98.9, df = 39, p < 0.0001), reducing by 18.3 Mg ha^{-1} CO_2 $month^{-1}$; in contrast, due to corresponding decreases in both GPP and R_{eco}, NEE did not change significantly over time at OPmature (f = 2.2, df = 25, p = 0.16). Table 1 shows NEE for individual 12-month periods captured at both study sites.

3.3 | Soil organic carbon loss (as CO_2-C) for individual study years at both sites

The ΔSOC was 2.5 to three times higher in OPnew compared to OPmature (Table 1). The sequestration rate of carbon into the extant biomass pool (NPP) increased between years 1 and 3 of the study at OPnew from 0.8 ± 0.07 Mg CO_2-C ha^{-1} $year^{-1}$ (plantation cycle months 5–16) to 2.3 ± 0.3 Mg CO_2-C ha^{-1} $year^{-1}$ (months 29–40). At OPmature, NPP declined slightly over the 2 years of monitoring, from 7.2 ± 2.7 Mg CO_2-C ha^{-1} $year^{-1}$ (plantation cycle months 119–130) to 6.8 ± 3.0 Mg CO_2-C ha^{-1} $year^{-1}$ (months 131–142). The estimated contribution of respiration from the decomposition of forest biomass (R_{fr}) to gross ecosystem respiration (R_{eco}) over the study periods at each site reduced from a mean of 19% at OPnew to 1.5% at OPmature.

3.4 | Chronosequence of cumulative NEE

Total cumulative NEE across the entire chronosequence suggested a net emission of CO_2 from the site at 823.3 ± 0.9 Mg CO_2 ha^{-1} (224.9 ± 0.2 Mg CO_2-C ha^{-1}) after 151 months. As can be seen in Figure 3, interpolating across the missing months in the OPmature data set (months 141–146) suggested the system might have been showing a net monthly uptake during this period which would

TABLE 1 Annual carbon fluxes and biomass uptake (Mg CO_2-C ha^{-1} $year^{-1}$) for complete measurement years during the study period and resulting estimates of changes in soil organic carbon (ΔSOC) calculated using Equation (4)

Site	OPnew	OPnew	OPnew	OPmature	OPmature
Sampling period	Sep 16 to Aug 17	Sep 17 to Aug 18	Sep 18 to Aug 19	May 17 to Apr 18	May 18 to Apr 19
Plantation cycle months	5–16	17–28	29–40	119–130	131–142
ΔSOC	−33.4 ± 7.5	−28.3 ± 1.3	−29.2 ± 1.8	−11.3 ± 2.7	−12.2 ± 3.0
R_{fr}	13.9 ± 0.7	10.4 ± 0.6	7.7 ± 0.4	0.8 ± 0.04	0.6 ± 0.03
GPP	9.9 ± 7.4	19.7 ± 1.1	26.2 ± 1.8	44.1 ± 0.02	40.3 ± 0.05
R_{eco}	56.4 ± 0.03	57.4 ± 0.05	60.9 ± 0.05	49.00 ± 0.02	46.3 ± 0.02
NEE	46.5 ± 0.03	37.7 ± 0.03	34.7 ± 0.06	4.9 ± 0.05	6.0 ± 0.06
NPP	0.8 ± 0.07	1.0 ± 0.1	2.3 ± 0.3	7.2 ± 2.7	6.8 ± 3.0

Note: Mass units: Mg CO_2-C ha^{-1} $year^{-1}$ (± propagated SEM).

Abbreviations: GPP, gross primary productivity; NPP, net primary productivity; R_{eco}, total ecosystem respiration, NEE, net ecosystem exchange of carbon; R_{fr}, respiration of carbon from decomposition of forest residue; ΔSOC, changes in soil organic carbon during period.

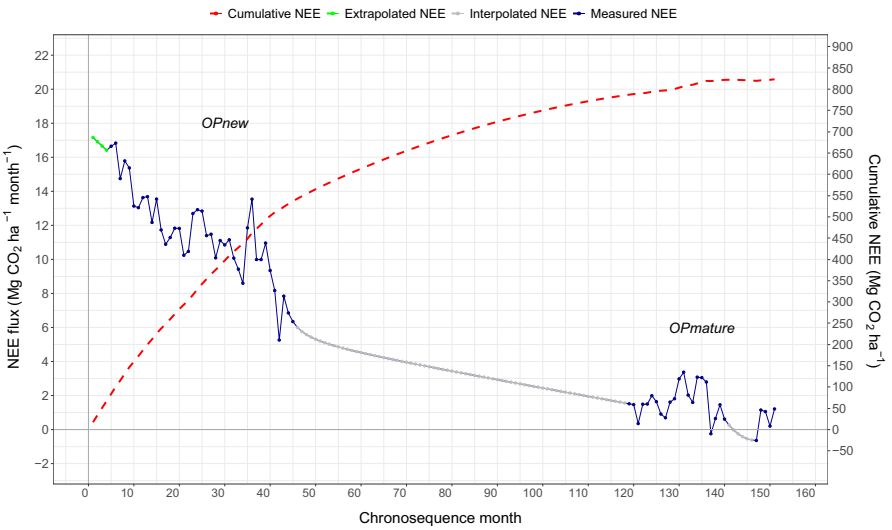

FIGURE 3 Monthly chronosequence plot of net ecosystem exchange of carbon (NEE), combining OPnew and OPmature into a single timeseries. Blue solid line shows measured monthly sums of NEE from each site plotted against month since respective plantation establishment. Dotted grey line shows interpolated monthly values, green line shows NEE extrapolated for the first 4 months at OPnew, dashed red line shows cumulative NEE summed from the resulting complete timeseries. Positive values (i.e. Y > 0) indicate a net emission of carbon from the ecosystem to the atmosphere, and negative values (i.e. Y < 0) indicate a net uptake

offset the rate of increase in NEE. This can be seen in the corresponding levelling off in the cumulative NEE curve beyond month 140. The first 4 months following conversion, extrapolated backwards from the beginning of monitoring at OPnew, month 5 (see Section 2), suggested total R_{eco} during that period of 68.8 Mg CO_2 ha^{-1} with GPP during the same 4-month period at 1.6 Mg CO_2 ha^{-1}. This resulted in an estimated net emission (NEE) of 67.2 ± 0.5 Mg CO_2 ha^{-1} over these first 4 months. Adding these months (1–4) to the beginning of the monthly time series for OPnew (months 5–45) gave a net cumulative NEE by the end of the OPnew monitoring period at 536.7 ± 0.6 Mg CO_2 ha^{-1} (146.7 ± 0.2 Mg CO_2-C ha^{-1}).

3.5 | Annual carbon emission factors (as CO_2-C)

Mean annual NEE across the 151-month chronosequence showed a net annual emission of 17.9 ± 1.3 Mg CO_2-C ha^{-1} $year^{-1}$ (65.6 ± 4.8 Mg CO_2 ha^{-1} $year^{-1}$). Using Equation (4) (modified by Equation 5) to account for carbon sequestered into on site biomass at a mean annual NPP of 4.9 ± 0.2 Mg CO_2-C ha^{-1} $year^{-1}$ and a mean annual carbon emission from the decomposition of forest residue (R_{fr}) at 4.6 ± 0.1 Mg CO_2-C ha^{-1} suggested a mean ΔSOC over the entire period at −18.3 ± 1.3 Mg CO_2-C ha^{-1} $year^{-1}$ (equivalent to a soil surface emission of 67 ± 4.8 Mg CO_2 ha^{-1} $year^{-1}$).

For years 1–6 (months 1–72), mean annual NEE was 30.2 ± 0.1 Mg CO_2-C ha^{-1} $year^{-1}$, mean annual NPP was 2.9 ± 1.3 Mg CO_2-C ha^{-1} $year^{-1}$ and R_{fr} was 8.1 ± 0.2 Mg CO_2-C ha^{-1} $year^{-1}$ which resulted in an early years' emission factor for peat carbon at −24.9 ± 1.3 Mg CO_2-C ha^{-1} $year^{-1}$ (91.4 ± 4.8 Mg CO_2 ha^{-1} $year^{-1}$).

This was much reduced for years 7–12 (months 73–144), with NEE at 7.2 ± 0.4 Mg CO_2-C ha^{-1} $year^{-1}$, NPP at 6.9 ± 6.1 Mg CO_2-C ha^{-1} $year^{-1}$ and R_{fr} at 1.4 ± 0.01 which resulted in a mature phase emission factor of −12.8 ± 6.1 Mg CO_2-C ha^{-1} $year^{-1}$ (46.9 ± 22.3 Mg CO_2 ha^{-1} $year^{-1}$). Table 2 shows annual and cumulative components for the chronosequence (NEE, NPP and R_{fr}) with the resulting estimates of ΔSOC for years 1–12 (months 1–144).

3.6 | Linear fit of ΔSOC (as CO_2 flux) to WTD

Adding our sites' annual soil carbon emissions (ΔSOC in Table 1, as CO_2) and mean WTD (see Figure 4) to the Hooijer et al. (2010) data set increased the model coefficient to CO_2 = 118.1 ± 14.5 x WTD (m), with a highly significant fit (F = 66.48, df = 12, p < 0.0001). Allowing the intercept to solve gave a model fit of CO_2 = 7.4 + 105.6 × WTD (m) but only the slope was found to be significant (p = 0.04). Excluding the very high fluxes seen from the conversion period at OPnew, by including only fluxes from OPmature (see Figure S.1.5), resulted in a model fit in close agreement with the original Hooijer et al. (2010) analysis with a highly significant model fit at CO_2 = 93.7 ± 9.8 × WTD (m; F = 91.4, df = 9, p < 0.0001).

TABLE 2 Chronosequence estimates of the change in soil organic carbon and individual components of the mass balance equation (Equation 4 modified by Equation 5) for individual years up to year 12 (months 1–144) and cumulatively over this period

Plantation cycle year	1	2	3	4	5	6	7	8	9	10	11	12
NEE annual	50.9 ± 0.2	39.2 ± 0.03	36.2 ± 0.04	25.2 ± 0.08	16.2 ± 0.08	13.6 ± 0.06	11.5 ± 0.05	9.5 ± 0.04	7.6 ± 0.04	5.7 ± 0.03	5.6 ± 0.05	3.4 ± 0.05
NEE cumulative	50.9 ± 0.2	90.1 ± 0.2	126.2 ± 0.2	151.4 ± 0.2	167.5 ± 0.2	181.1 ± 0.2	192.7 ± 0.2	202.2 ± 0.2	209.8 ± 0.2	215.5 ± 0.2	221.0 ± 0.2	224.5 ± 0.2
NPP annual	0.7 ± 0.1	1.0 ± 0.3	1.2 ± 0.5	4.6 ± 1.2	4.9 ± 2.3	5.1 ± 3.4	6.1 ± 4.5	6.4 ± 5.6	6.9 ± 6.0	6.8 ± 6.3	7.9 ± 6.8	7.6 ± 7.3
NPP cumulative	0.7 ± 0.1	1.7 ± 0.3	2.9 ± 0.6	7.5 ± 1.3	12.4 ± 2.7	17.4 ± 4.3	23.5 ± 6.2	29.9 ± 8.3	36.8 ± 10.3	43.6 ± 12.1	51.5 ± 13.8	59.1 ± 15.7
R_{fr} annual	15.0 ± 0.7	11.2 ± 0.4	8.3 ± 0.2	6.2 ± 0.1	4.6 ± 0.06	3.4 ± 0.04	2.6 ± 0.02	1.9 ± 0.01	1.4 ± 0.01	1.1 ± 0.003	0.8 ± 0.002	0.6 ± 0.001
R_{fr} cumulative	15.0 ± 0.7	26.2 ± 0.8	34.5 ± 0.8	40.7 ± 0.8	45.3 ± 0.8	48.8 ± 0.8	51.3 ± 0.8	53.2 ± 0.8	54.6 ± 0.8	55.6 ± 0.8	56.4 ± 0.8	57.0 ± 0.8
ΔSOC annual	−36.6 ± 0.7	−29.0 ± 0.5	−29.0 ± 0.5	−23.6 ± 1.2	−16.4 ± 2.3	−15.3 ± 3.4	−15.0 ± 4.5	−14.0 ± 5.6	−13.1 ± 6.0	−11.4 ± 6.3	−12.6 ± 6.8	−10.5 ± 7.3
ΔSOC cumulative	−36.6 ± 0.7	−65.6 ± 0.9	−94.6 ± 1.0	−118.2 ± 1.6	−134.6 ± 2.8	−149.8 ± 4.4	−164.9 ± 6.3	−178.9 ± 8.4	−192.00 ± 10.3	−203.4 ± 12.1	−216.0 ± 13.9	−226.5 ± 15.7

Note: Mass units: Mg CO_2-C ha^{-1} $year^{-1}$ (± propagated SEM).

Abbreviations: NEE, net ecosystem exchange of carbon; NPP, net primary productivity; R_{fr}, forest residue decomposition; units are mass of carbon, Mg CO_2-C ha^{-1}; ΔSOC, change in soil organic carbon over period.

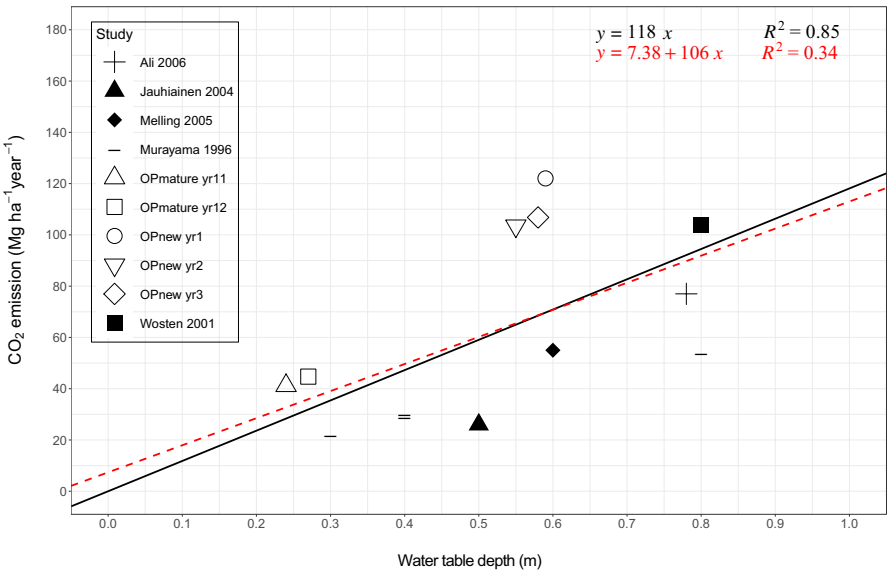

FIGURE 4 Recreation of Hooijer et al. (2010) linear fit of CO_2 emission to water table depth (closed symbols) with the inclusion of individual years from OPnew and OPmature (open symbols). Solid black line shows linear fit with intercept constrained to zero, dashed red line shows linear fit with intercept free. The effect of excluding the early years of very high emission at OPnew can be seen in Supporting Information (Figure S.1.5.); units are presented as CO_2 as in the original Hooijer analysis, these may be converted to CO_2-C (carbon) through multiplying by a factor of 12/44

TABLE 3 Modelled relationship between ecosystem respiration (R_{eco}) and water table depth (WTD)

WTD (m)	Annual Reco (CO_2-C) (Mg ha^{-1} $year^{-1}$)	Flux relative to WTD 0.6 m (%)
0	22.2 ± 4.8	40.4
0.1	30.8 ± 2.9	55.8
0.2	38.0 ± 1.6	69.1
0.3	44.1 ± 1.0	80.1
0.4	49.0 ± 1.1	89.0
0.5	52.7 ± 1.1	95.6
0.6	55.1 ± 1.0	100.0
0.7	56.3 ± 1.2	102.3
0.8	56.4 ± 2.1	102.3

Note: ± indicates the 95% confidence interval of the model fit.

3.7 | Non-linear fit of ecosystem respiration to WTD

The second-order polynomial fit of night-time R_{eco} to WTD (see Figure S.1.6.) was highly significant with an adjusted R^2 of 0.83 (F = 157.6, df = 64, p < 0.0001). Model coefficients across the range of WTD found at OPnew (0–0.8 m below the surface, binned into 0.1 m increments) predicted a 154% increase in annual R_{eco} when moving from the shallowest WTD (0 m) to the deepest (0.8 m). Table 3 shows predicted annual R_{eco} for each 0.1 m WTD increment and their magnitude relative to a typical plantation drainage target of 0.6 m. Figure 5 shows a graphical representation of these estimated percentage changes in annual R_{eco} when comparing different mean annual WTDs. For example, raising WTD to 0.2 m would see a 31% reduction in respiration compared to the typical 0.6 m target. In

Existing mean annual water table depth (m) \ New mean annual water table depth (m)	0	0.1	0.2	0.3	0.4	0.5	0.6	0.7	0.8
0	0	+38	+71	+99	+120	+137	+148	+153	+154
0.1	−28	0	+24	+43	+59	+71	+79	+83	+83
0.2	−42	−19	0	+16	+29	+38	+45	+48	+48
0.3	−50	−30	−14	0	+11	+19	+25	+28	+28
0.4	−55	−37	−22	−10	0	+7	+12	+15	+15
0.5	−58	−42	−28	−16	−7	0	+5	+7	+7
0.6	−60	−44	−31	−20	−11	−4	0	$+2^{ns}$	$+2^{ns}$
0.7	−61	−45	−32	−22	−13	−7	-2^{ns}	0	0^{ns}
0.8	−61	−45	−33	−22	−13	−7	-2^{ns}	0^{ns}	0

All crosswise comparisons are significantly different to each other at the 95% confidence interval except where stated as zero or not significant (ns)

FIGURE 5 Relative change (%) in soil carbon emission following a change from an existing mean annual water table depth (WTD) below the peat surface to a new target depth. Negative (green) values indicate a reduction, positive (orange) indicate an increase, ns (grey) values indicate changes that are not statistically significant. For example, changing from 0.4 m WTD (horizontal row) to 0.3 m (vertical column) would results in a 10% reduction in soil carbon emission (intersect at −10)

contrast, differences between depth increments deeper than 0.6 m were insignificant.

4 | DISCUSSION

4.1 | CO_2 flux

We have presented, for the first time, a comparative study of measured NEE of carbon as CO_2 between the initial years of peatland conversion to oil palm and the later mature phase. Our results show the dramatic difference between the very high early conversion period annual emission of CO_2 to the atmosphere at 137.8 Mg CO_2 ha^{-1} $year^{-1}$, and the mature phase emission at 17.5 Mg CO_2 ha^{-1} $year^{-1}$. Our mature phase figure for NEE is reasonably consistent with the estimated value for mature peatland of 12.1 ± 10.2 Mg CO_2 ha^{-1} $year^{-1}$ from Meijide et al. (2020), though less than half the 36.4 Mg CO_2 ha^{-1} $year^{-1}$ measured by Kiew et al. (2020) at their mature peatland plantation. Our 151-month chronosequence demonstrated that while the much lower NEE in later years might level off the rate of increase in cumulative NEE, it was highly unlikely to offset that cumulative carbon emission over a plantation lifetime. Recouping the total emissions over our chronosequence period (around 800 Mg CO_2 ha^{-1}) would require an average net uptake of ~100 Mg CO_2 ha^{-1} $year^{-1}$ for the remaining 7.5 years of a typical 20-year plantation lifetime.

While our results show that conversion may be adding around 110 Mg CO_2 ha^{-1} $year^{-1}$ (30.2 Mg CO_2-C ha^{-1} $year^{-1}$) to the atmosphere in the first 6 years of the conversion (months 1–72), not all of this would be coming directly from soil carbon decomposition. Our simple forest decomposition model suggested that around a quarter of this net emission could have been coming from CO_2 released by the decay of forest biomass. In contrast, while NEE had dropped to around 26 Mg CO_2 ha^{-1} $year^{-1}$ over the next 6 years (months 73–144), soil carbon emission remained high at around 47 Mg CO_2 ha^{-1} $year^{-1}$ but was being masked by NPP. Sequestration of carbon into the biomass pool (NPP) was equivalent to around 54% of the peat carbon loss for that period. A small proportion of that carbon will be contained within the fruit harvest offtake, removed from the site and returned to the atmosphere during oil production and consumption, the remainder will be held within the palm and frond litter biomass pool until re-cultivation (typically at around year 20) where it will begin to return to the atmosphere during the decomposition of the palm biomass following clearance.

We also considered the relative contributions to NEE from uptake (GPP) and emission (R_{eco}). The common approach for partitioning NEE (Reichstein et al., 2005) uses parameterization of the relationship between night-time NEE (assumed to be entirely R_{eco}) and air temperature to estimate the contribution of R_{eco} to daytime NEE (the residual being GPP). However, this approach relies on a strong relationship between respiration and temperature. This can be problematic in tropical climates where temperature ranges (both diurnally and seasonally) tend to be very much narrower than in temperate zones, and likely compounded by the strong relationship in drained peatlands between R_{eco} and WTD. As an alternative, we adopted the approach of Lasslop et al. (2010) using a light response curve fitted to daytime NEE to estimate GPP. Kiew et al. (2020) concluded that low GPP in their poorly established plantation was responsible for their large on site net emissions. In line with their conclusion, as seen in Figure 2, while R_{eco} was slightly lower at our mature site compared to OPnew, it was the much higher GPP into the mature palms that was primarily responsible for driving this reduction in NEE. There was a small, but statistically significant, reduction in both GPP and R_{eco} over time during the OPmature monitoring period, which appears to be most apparent in the period between August 2018 and February 2019. This dip in activity appears to have recovered at some point during our missing data period between then and September 2019. Stiegler et al. (2019) showed that drought conditions resulting from an El Nino-Southern Oscillation (ENSO) event in 2015 led to reduced CO_2 uptake into their study site at an Indonesian oil palm plantation. This might suggest that another ENSO event in the region, recorded between September 2018 and June 2019 (https://www.metoffice.gov.uk/research/climate/seasonal-to-decadal/gpc-outlooks/el-nino-la-nina), could be linked to our indication of a drop-off in photosynthetic activity. The later period of this ENSO event also coincided with a particularly bad period of air pollution haze due to extensive vegetation burning across the entire region (https://www.bbc.co.uk/news/world-asia-34265922), which may also have contributed to this. Monthly yield data from the site (not published) suggest a corresponding dip in FFB harvest during this period which might corroborate this, though more detailed analysis would be required to reach any firm conclusion.

4.2 | Relationship between WTD and soil carbon loss (as CO_2)

Adding our estimate of soil carbon loss (as CO_2) from OPmature to the Hooijer et al. (2010) linear regression model, we found that our mature site fitted remarkably well within their original data set, only raising the coefficient to 93.7 from their CO_2 = 91*WTD. However, including our early conversion period at OPnew increased this sensitivity estimate by 26%. This reinforces the importance of incorporating the early years of conversion into assessments of the carbon impacts of peatland conversion and emphasizes the need for emission factors covering entire cropping periods.

A single coefficient such as this may, though, be too simplistic. As discussed in Hooijer et al. (2006), a coefficient for the relationship between CO_2 flux and WTD is unlikely to be consistent throughout the soil profile, and it was a lack of available data which limited their original analysis to a simple linear fit. In their discussion (see note under figure 12 in Hooijer et al. (2006)), the authors suggest that CO_2 emissions might be reduced at WTD of 0.2–0.3 m and at zero when WTD = 0, that is, waterlogged conditions would promote the formation of peat and net CO_2 emissions would <= 0. Their suggestion that a linear coefficient of 91 would hold true for WTD from

0.25 and 1.1 m was discussed in Couwenberg et al., 2010) who concluded that there was not enough evidence to clearly state whether rates of subsidence (as a measure of peat decomposition) became static beyond a WTD of 0.5 m.

Taking advantage of our high-frequency, long-term data set at OPnew, where heterotrophic respiration should heavily outweigh the limited autotrophic respiration from immature, widely spaced palms, we investigated this relationship using a non-linear, polynomial fit. Here we found not only a highly significant relationship (in contrast to Cooper et al., 2020, whose study had very little regression data available) but one that implied the opposite to what was suggested in Hooijer et al. (2006). We found a much greater sensitivity to drainage in the upper half of the soil profile compared to the lower half over our 0–0.8 m WTD range (see Table 3). Each additional 0.1 m drainage within the upper 0.4 m produced an additional 24.5 Mg CO_2 ha^{-1} $year^{-1}$ (compared to 9.1 Mg CO_2 ha^{-1} $year^{-1}$ expected from Hooijer et al. (2010)), while between 0.5 and 0.8 m this decreased to 6.8 Mg CO_2 ha^{-1} $year^{-1}$. This trend may be reasonably intuitive, Leifeld et al. (2012) showed that peat decomposition rates were dependent on organic matter quality and that decomposability was higher in the newer organic matter nearer the peat surface. Given the importance of temperature in driving soil carbon decomposition (Lloyd & Taylor, 1994), it would also follow that the drained upper layers (with a corresponding decrease in soil heat capacity) would see greater (and faster) soil temperature responses to incoming solar radiation, again suggesting that we might expect this greater sensitivity of respiration to drainage in the upper profile. While our results (Figure 5) are only from a single site, they do indicate the potential impact (and significant carbon conservation) that might be achieved through more strategic management of water table in the upper soil layers. However, more work is needed to investigate the impact that reducing WTD would have on fruit yield.

4.3 | Comparison to subsidence studies

Hooijer et al. (2012) estimated (from subsidence studies) that the first 5 years of conversion from PSF to plantation (acacia as this is the conversion they used to estimate 0–5 year fluxes) would see a mean loss of peat carbon at 48.6 Mg CO_2-C ha^{-1} $year^{-1}$ (calculated from CO_{2eq}. figures in their Table 2); our estimate for OPnew mean peat carbon loss was considerably lower than this at 30.3 Mg CO_2-C ha^{-1} $year^{-1}$ over the first 3 years. For mature oil palm sites (>6 years) they suggest a mean annual loss of 19.9 Mg CO_2-C ha^{-1} $year^{-1}$ at a mean WTD of 0.71 m (therefore CO_{2eq}. = 102.6*WTD [m]), a figure in close agreement with a modelled range of 18–22 Mg CO_2-C ha^{-1} $year^{-1}$ at WTD of 0.7 m given in Carlson et al. (2015). The OPmature site in our study (years 11 and 12) again showed a lower carbon loss than this at only 11.7 Mg CO_2-C ha^{-1} $year^{-1}$. However, mean WTD at OPmature was much closer to the soil surface (0.26 m) than in the Hooijer et al. (2012) analysis, which gives a relationship of CO_2 = 164.7*WTD (m), around 60% higher, which might be expected from our comparison between the polynomial and linear fits discussed above.

Hooijer et al. (2012) estimated a long-term (years 0–18) mean annual carbon loss of 32.5 Mg CO_2-C ha^{-1} $year^{-1}$, a figure that agrees well with an annualized 20-year figure of 29 Mg CO_2-C ha^{-1} $year^{-1}$ calculated through literature review by Page et al. (2011). These values are both heavily influenced by the inclusion of very high peat carbon emissions in the early years estimated from observed rapid initial subsidence. Our chronosequence estimate of mean annual soil carbon loss (over 12 years) was 35% lower than this at 18.9 Mg CO_2-C ha^{-1} $year^{-1}$, a figure in very close agreement to the mean annual carbon loss for conversions estimated in Couwenberg and Hooijer (2013) at 18 Mg CO_2-C ha^{-1} $year^{-1}$, a study aimed at improving the methodology for subsidence estimates of carbon loss from peatland- conversions. However, this later study assumed, but did not account for, peat carbon losses in the early years being far higher and the figure of 18 Mg ha^{-1} $year^{-1}$ was recommended only for mature conversions in a 'steady state'. Our results for the early years, which are twice the mature value, are included in our 12-year estimate, suggesting, from our sites at least, that including these early years does not raise the mean emission beyond the Couwenberg and Hooijer (2013) estimate. However, we must acknowledge that drainage at our mature site particularly may not have been as effective as site managers would typically prefer. A recent meta-analysis (Prananto et al., 2020) showed a mean WTD across 138 tropical peatland plantations at 0.56, 0.3 m deeper than our mean for OPmature (0.26 m). With reference to Figure 5, increasing WTD from 0.3 to 0.6 m below the surface could see an increase in CO_2 emission of up to 25%, suggesting that emissions for OPmature may be lower than might be expected from deeper drained plantations.

It should also be noted that our estimate of CO_2 flux from the decomposition of the forest biomass was contributing around a quarter of the total ecosystem CO_2 emission to the atmosphere (R_{eco}). This contribution would be reducing the estimate of early years' peat decomposition considerably in our mass balance equation, 75% of the forest residue was decomposed within 4 years in our decomposition model. This estimate was based on a literature figure for the starting biomass (Kho & Jepsen, 2015) and an assumption that 25% had decomposed by the end of the first year from a single decomposition study (Law et al., 2019). Our decomposition rate can be compared to a study carried out under similar climatic conditions in Panama, South America (Hoyos-Santillan et al., 2015), which reported 44% of starting biomass remaining after 2 years (stems up to 0.05 m diameter, when left aboveground), our chosen decay constant would result in 55% remaining after the same period. Given that our assumption includes CWD over a range of diameters, including much larger than 0.05 m, this might seem a reasonable value, however it is an assumption. Any decrease in decomposition rate or starting biomass would have a corresponding increase in the estimate of SOC loss for these early years. Our sensitivity analysis (see Supporting Information S.2) showed that while adjusting these values did have this impact on

estimates of ΔSOC, particularly in the early years, even at unrealistic levels they did not bring emissions from our sites to the levels suggested in subsidence studies. Uncertainty levels were also high in our estimate of NPP and increased over time with propagation of all the uncertainties in individual vegetation component assessments. Again, the implications of this can be seen in our sensitivity analysis in Table S.2.2 where we consider the impact of doubling our estimate of NPP across a range of residue decomposition rate scenarios. Even at our lowest decomposition rate and doubled NPP, our long-term estimate of peat carbon loss remained 18% lower than the corresponding subsidence estimate.

An aspect not captured in our direct monitoring of the ecosystem/atmosphere exchange of CO_2 is peat loss due to the export of carbon in groundwater as dissolved and particulate organic carbon. This is represented within ε in Equation (4) and is something that would be captured in subsidence studies. A recent paper (Cook et al., 2018) investigated fluvial carbon losses from study sites in the same plantation estates as our current study and reported losses of organic carbon in the range of 0.3–0.5 Mg ha^{-1} $year^{-1}$. This would add around 2.5% to our estimated peat organic carbon loss but would not raise it to the levels expected in Hooijer et al. (2012) or Page et al. (2011). Similarly, consideration needs to be given to potential emissions of soil carbon as CH_4 even though, as reported in Couwenberg et al. (2009), CH_4 emissions from tropical peatlands are typically far lower than those from boreal/temperate peatlands. Manning et al. (2019) monitored CH_4 emission from soils (and drainage channels) at the Sabaju and Sebungan plantations (though from different planting blocks to our OPnew and OPmature) and, as with their CO_2 results, found fluxes from Sabaju (0.03 Mg CH_4-C ha^{-1} $year^{-1}$) to be higher than from Sebungan (0.006 Mg CH_4-C ha^{-1} $year^{-1}$). While the GWP impact of CH_4 is calculated at 34 times that of CO_2 (Myhre et al. 2013), in terms of soil carbon loss, this level of carbon mobilization would add only around 0.1% to our estimate of annual carbon loss over the entire chronosequence (increasing to around 0.3% if drainage water CH_4-C emissions were included).

4.4 | Comparison to existing emission factors (as CO_2)

Our long-term emission factor (calculated across all 151 months) for peat carbon loss (as CO_2) at 67 Mg CO_2 ha^{-1} $year^{-1}$ is closer to the IPCC emission factor for peatland conversion to acacia plantation, 73 Mg CO_2 ha^{-1} $year^{-1}$ than oil palm which is lower at 40 Mg CO_2 ha^{-1} $year^{-1}$ (Hiraishi et al., 2014). The effect of plantation species on peatland CO_2 emission was not found to be a significant factor in the study of Carlson et al. (2015), who discussed the likely importance of time since drainage, though their data set was limited to a narrow age range. Miettinen et al. (2017) preferred to use the mean of the two IPCC factors (55 Mg CO_2 ha^{-1} $year^{-1}$), in their calculation of carbon loss across the region due to peatland conversion which agrees well with the Cooper et al. (2020) mean figure of 53.1 Mg CO_2 ha^{-1} $year^{-1}$. All these estimates remain lower than the EPA-accepted emission factor of 95 Mg CO_2 ha^{-1} $year^{-1}$ (EPA, 2014). The IPCC explicitly exclude the first 6 years of conversion in their emission factor due to lack of data but acknowledge that this period would see much higher carbon losses. This is clearly demonstrated by our estimate of soil carbon emission for years 1–6 at 91.6 Mg CO_2 ha^{-1} $year^{-1}$. The overall net emission of CO_2 to the atmosphere (NEE) for this period, incorporating forest biomass decomposition and photosynthetic uptake, was higher at 110.8 Mg CO_2 ha^{-1} $year^{-1}$.

This difference between direct soil carbon emission (ΔSOC, as CO_2) and the net ecosystem scale addition of CO_2 to the atmosphere (NEE) is an important distinction, particularly in the early years of conversion, and should be considered when assessing the impacts of land-use change. In Table 2, we present, based on our results, estimates of emission factors for both NEE and ΔSOC at an annual time step across a 12-year period. Taking the cumulative sum (for either component) for any given period and dividing by that number of years will provide an estimate of mean annual CO_2 emission for that period.

5 | CONCLUSIONS

Despite our results reporting lower peat carbon loss in the early years following conversion than subsidence studies might have suggested, there is no doubt that these emissions remain extremely significant and PSF conversion to agriculture results in very large net emissions of CO_2. We have shown that the impact of these fluxes on the atmospheric carbon pool can be larger than emission factors for soil carbon loss alone might suggest, and that is highly unlikely that 'carbon debts' incurred early in a plantation lifecycle could be recouped over the remaining years. Evidence has shown that moratoria on peatland conversion within protected areas can be effective (Chen et al., 2019) but huge challenges remain, and newly identified areas of extensive peatland being reported from tropical zones across the globe (Lähteenoja & Page, 2011; Xu et al., 2018) reveal regions that may be particularly vulnerable to land-use change. Despite policy development in South East Asia, limitations in regulatory frameworks and enforcement capabilities combined with political and socio-economic factors still challenge peatland protection (Padfield et al., 2016; Wijedasa et al., 2018). Our results should make it clear that conservation of these globally important carbon stocks is vital to any efforts to minimize the impacts of future climate change and reduce the contribution of land-use change to it.

ACKNOWLEDGEMENTS

The authors thank the Director-General of the Malaysian Palm Oil Board (MPOB) for permission to publish these results. This study was carried out as part of a wider tropical peat research collaboration between MPOB, University of Exeter, University of Aberdeen and Newcastle University, and they thank the Sarawak Oil Palm Berhard (SOPB) for their help and support during the project.

Specifically, at SOPB they thank Paul Wong Hee Kwong (group CEO), Chua Kian Hong (group plantation manager), Phang Seng Nam (regional plantation controller) and the Sabaju and Sebungan plantation managers for being kind enough to allow the research platform to be established within their plantations and for providing logistical support when needed. At MPOB, they particularly thank the dedicated field technicians, without whose efforts and commitment the research would not have been possible, specifically Ham Jonathon, Muhammad Amira Ruzaizul Bin Bujang and Steward Saging. Finally, they thank Professors Susan Page (Leicester University, International Advisory Panel for the project), Takashi Hirano (Hokkaido University, International Advisory Panel) and Christopher Evans (Centre for Ecology and Hydrology, Bangor, UK) for providing comments and suggestions during the development of the manuscript.

CONFLICT OF INTEREST

The research was carried out as part of a project funded by the Malaysian Palm Oil Board (MPOB). L. K. K and E. R. are both employees of MPOB. The research was carried out with the support of Sarawak Oil Palm Berhard (SOPB) on whose land the research project was based.

DATA AVAILABILITY STATEMENT

The data that support the findings of this study are available from the corresponding author upon reasonable request.

ORCID

Jon McCalmont https://orcid.org/0000-0002-5978-9574

REFERENCES

Baldocchi, D. D. (2003). Assessing the eddy covariance technique for evaluating carbon dioxide exchange rates of ecosystems: Past, present and future. *Global Change Biology*, *9*, 479–492. https://doi.org/10.1046/j.1365-2486.2003.00629.x

Baldocchi, D., Falge, E., Gu, L., Olson, R., Hollinger, D., Running, S., Anthoni, P., Bernhofer, C., Davis, K., & Evans, R. (2001). FLUXNET: A new tool to study the temporal and spatial variability of ecosystem-scale carbon dioxide, water vapor, and energy flux densities. *Bulletin of the American Meteorological Society*, *82*, 2415–2434. https://doi.org/10.1175/1520-0477(2001)082<2415:fantts>2.3.co;2

Carlson, K. M., Goodman, L. K., & May-Tobin, C. C. (2015). Modeling relationships between water table depth and peat soil carbon loss in Southeast Asian plantations. *Environmental Research Letters*, *10*. https://doi.org/10.1088/1748-9326/10/7/074006

Cheng, W. (2009). Rhizosphere priming effect: Its functional relationships with microbial turnover, evapotranspiration, and C-N budgets. *Soil Biology and Biochemistry*, *41*, 1795–1801. https://doi.org/10.1016/j.soilbio.2008.04.018

Cheng, Y., Yu, L., Xu, Y., Liu, X., Lu, H., Cracknell, A. P., Kanniah, K., & Gong, P. (2018). Towards global oil palm plantation mapping using remote-sensing data. *International Journal of Remote Sensing*, *39*, 5891–5906. https://doi.org/10.1080/01431161.2018.1492182

Chen, B., Kennedy, C. M., & Xu, B. (2019). Effective moratoria on land acquisitions reduce tropical deforestation: Evidence from Indonesia. *Environmental Research Letters*, *14*, 044009. https://doi.org/10.1088/1748-9326/ab051e

Cook, S., Whelan, M. J., Evans, C. D., Gauci, V., Peacock, M., Garnett, M. H., Kho, L. K., Teh, Y. A., & Page, S. E. (2018). Fluvial organic carbon fluxes from oil palm plantations on tropical peatland. *Biogeosciences*, *15*, 7435–7450. https://doi.org/10.5194/bg-15-7435-2018

Cooper, H. V., Evers, S., Aplin, P., Crout, N., Dahalan, M. P. B., & Sjogersten, S. (2020). Greenhouse gas emissions resulting from conversion of peat swamp forest to oil palm plantation. *Nature Communications*, *11*, 1–8. https://doi.org/10.1038/s41467-020-14298-w

Couwenberg, J., Dommain, R., & Joosten, H. (2009). Greenhouse gas fluxes from tropical peatlands in south-east Asia. *Global Change Biology*, *16*, 1715–1732. https://doi.org/10.1111/j.1365-2486.2009.02016.x

Couwenberg, J., & Hooijer, A. (2013). Towards robust subsidence-based soil carbon emission factors for peat soils in south-east Asia, with special reference to oil palm plantations. *Mires & Peat*, *12*, 10–14. https://doi.org/10.1016/s0269-915x(98)80095-5

Dariah, A., Marwanto, S., & Agus, F. (2014). Root-and peat-based CO_2 emissions from oil palm plantations. *Mitigation and Adaptation Strategies for Global Change*, *19*, 831–843. https://doi.org/10.1007/s11027-013-9515-6

Environmental Protection Agency (EPA) (2014). *Emission Factor for Tropical Peatlands Drained for Oil Palm Cultivation Peer – Review Report*. Washington, D.C.

Falge, E., Baldocchi, D., Olson, R., Anthoni, P., Aubinet, M., Bernhofer, C., Burba, G., Ceulemans, R., Clement, R., & Dolman, H. (2001). Gap filling strategies for defensible annual sums of net ecosystem exchange. *Agricultural and Forest Meteorology*, *107*, 43–69. https://doi.org/10.1016/s0168-1923(00)00225-2

Foken, T., Göockede, M., Mauder, M., Mahrt, L., Amiro, B., & Munger, W. (2004). Post-field data quality control. In X. Lee, W. Massman, & B. Law (Eds.), *Handbook of micrometeorology*. Atmospheric and Oceanographic Sciences Library (Vol. *29*, pp. 181–208). Dordrecht: Springer. https://doi.org/10.1007/1-4020-2265-4_9

Friedlingstein, P., Jones, M., O'Sullivan, M., Andrew, R., Hauck, J., Peters, G., Peters, W., Pongratz, J., Sitch, S., & le Quéré, C. (2019). Global carbon budget 2019. *Earth System Science Data*, *11*, 1783–1838.

Gaveau, D. L., Locatelli, B., Salim, M. A., Yaen, H., Pacheco, P., & Sheil, D. (2018). Rise and fall of forest loss and industrial plantations in Borneo (2000–2017). *Conservation Letters*, *12*(3), e12622. https://doi.org/10.1111/conl.12622

Hergoualc'h, K., Hendry, D. T., Murdiyarso, D., & Verchot, L. V. (2017). Total and heterotrophic soil respiration in a swamp forest and oil palm plantations on peat in Central Kalimantan, Indonesia. *Biogeochemistry*, *135*, 203–220. https://doi.org/10.1007/s10533-017-0363-4

Hill, T., Chocholek, M., & Clement, R. (2017). The case for increasing the statistical power of eddy covariance ecosystem studies: Why, where and how? *Global Change Biology*, *23*, 2154–2165. https://doi.org/10.1111/gcb.13547

Hiraishi, T., Krug, T., Tanabe, K., Srivastava, N., Baasansuren, J., Fukuda, M., & Troxler, T. (2014). *2013 supplement to the 2006 IPCC guidelines for national greenhouse gas inventories: Wetlands*. IPCC.

Hirano, T., Segah, H., Kusin, K., Limin, S., Takahashi, H., & Osaki, M. (2012). Effects of disturbances on the carbon balance of tropical peat swamp forests. *Global Change Biology*, *18*, 3410–3422. https://doi.org/10.1111/j.1365-2486.2012.02793.x

Hooijer, A., Page, S., Canadell, J. G., Silvius, M., Kwadijk, J., Wösten, H., & Jauhiainen, J. (2010). Current and future CO_2 emissions from drained peatlands in Southeast Asia. *Biogeosciences*, *7*, 1505–1514. https://doi.org/10.5194/bg-7-1505-2010

Hooijer, A., Page, S., Jauhiainen, J., Lee, W., Lu, X., Idris, A., & Anshari, G. (2012). Subsidence and carbon loss in drained

tropical peatlands. *Biogeosciences*, *9*(3), 1053–1071. https://doi.org/10.5194/bg-9-1053-2012

Hooijer, A., Silvius, M., Wösten, H., Page, S., Hooijer, A., Silvius, M., Wösten, H., & Page, S. (2006). PEAT-CO2. In *Assessment of CO_2 emissions from drained peatlands in SE Asia*, *Delft Hydraulics report Q*, 3943. https://www.researchgate.net/publication/285726396_PEAT-CO2_assessment_of_CO2_emissions_from_drained_peatlands_in_SE_Asia

Houghton, R. A., & Nassikas, A. A. (2017). Global and regional fluxes of carbon from land use and land cover change 1850–2015. *Global Biogeochemical Cycles*, *31*, 456–472. https://doi.org/10.1002/2016gb005546

Hoyos-Santillan, J., Lomax, B. H., Large, D., Turner, B. L., Boom, A., Lopez, O. R., & Sjögersten, S. (2015). Getting to the root of the problem: Litter decomposition and peat formation in lowland Neotropical peatlands. *Biogeochemistry*, *126*, 115–129. https://doi.org/10.1007/s10533-015-0147-7

Ishikura, K., Hirano, T., Okimoto, Y., Hirata, R., Kiew, F., Melling, L., Aeries, E. B., San Lo, K., Musin, K. K., & Waili, J. W. (2018). Soil carbon dioxide emissions due to oxidative peat decomposition in an oil palm plantation on tropical peat. *Agriculture, Ecosystems & Environment*, *254*, 202–212. https://doi.org/10.1016/j.agee.2017.11.025

Kenney-Lazar, M., & Ishikawa, N. (2019). Mega-plantations in southeast Asia: Landscapes of displacement. *Environment and Society*, *10*, 63–82. https://doi.org/10.3167/ares.2019.100105

Khalid, H., Zin, Z., & Anderson, J. (1999). Quantification of oil palm biomass and nutrient value in a mature plantation. II. Below-ground biomass. *Journal of Oil Palm Research*, *11*, 63–71.

Kho, L. K., & Jepsen, M. R. (2015). Carbon stock of oil palm plantations and tropical forests in Malaysia: A review. *Singapore Journal of Tropical Geography*, *36*, 249–266. https://doi.org/10.1111/sjtg.12100

Kiew, F., Hirata, R., Hirano, T., Xhuan, W. G., Aries, E. B., Kemudang, K., Wenceslaus, J., San, L. K., & Melling, L. (2020). Carbon dioxide balance of an oil palm plantation established on tropical peat. *Agricultural and Forest Meteorology*, *295*, 108189. https://doi.org/10.1016/j.agrformet.2020.108189

Kljun, N., Calanca, P., Rotach, M., & Schmid, H. (2004). A simple parameterisation for flux footprint predictions. *Boundary-Layer Meteorology*, *112*, 503–523. https://doi.org/10.23919/ecc.1999.7099991

Kormann, R., & Meixner, F. X. (2001). An analytical footprint model for non-neutral stratification. *Boundary-Layer Meteorology*, *99*, 207–224.

Kuzyakov, Y. (2010). Priming effects: Interactions between living and dead organic matter. *Soil Biology and Biochemistry*, *42*, 1363–1371.

Lähteenoja, O., & Page, S. (2011). High diversity of tropical peatland ecosystem types in the Pastaza-Marañón basin, Peruvian Amazonia. *Journal of Geophysical Research: Biogeosciences*, 116. https://doi.org/10.1029/2010JG001508

Lasslop, G., Reichstein, M., Papale, D., Richardson, A. D., Arneth, A., Barr, A., Stoy, P., & Wohlfahrt, G. (2010). Separation of net ecosystem exchange into assimilation and respiration using a light response curve approach: Critical issues and global evaluation. *Global Change Biology*, *16*, 187–208. https://doi.org/10.1111/j.1365-2486.2009.02041.x

Law, S., Eggleton, P., Griffiths, H., Ashton, L., & Parr, C. (2019). Suspended dead wood decomposes slowly in the tropics, with microbial decay greater than termite decay. *Ecosystems*, *22*, 1176–1188.

le Quéré, C., Andrew, R. M., Friedlingstein, P., Sitch, S., Hauck, J., Pongratz, J., Pickers, P. A., Korsbakken, J. I., Peters, G. P., & Canadell, J. G. (2018). Global carbon budget 2018. *Earth System Science Data*, *10*, 2141–2194. https://doi.org/10.5194/essd-10-2141-2018

Leifeld, J., Steffens, M., & Galego-Sala, A. (2012). Sensitivity of peatland carbon loss to organic matter quality. *Geophysical Research Letters*, *39*. https://doi.org/10.1029/2012GL051856

Lewis, K., Rumpang, E., Kho, L. K., McCalmont, J., Teh, Y. A., Gallego-Sala, A., & Hill, T. C. (2020). An assessment of oil palm plantation aboveground biomass stocks on tropical peat using destructive and non-destructive methods. *Scientific Reports*, *10*, 1–12. https://doi.org/10.1038/s41598-020-58982-9

Lloyd, J., & Taylor, J. (1994). On the temperature dependence of soil respiration. *Functional Ecology*, *8*(3), 315–323.

Manning, F. C., Kho, L. K., Hill, T. C., Cornulier, T., & Teh, Y. A. (2019). Carbon emissions from oil palm plantations on peat soil. *Frontiers in Forests and Global Change*, *2*, 37–39. https://doi.org/10.1016/j.ancene.2018.04.004

Masseroni, D., Corbari, C., & Mancini, M. (2014). Limitations and improvements of the energy balance closure with reference to experimental data measured over a maize field. *Atmósfera*, *27*, 335–352. https://doi.org/10.1016/S0187-6236(14)70033-5

Mattsson, B., Cederberg, C., & Blix, L. (2000). Agricultural land use in life cycle assessment (LCA): Case studies of three vegetable oil crops. *Journal of Cleaner Production*, *8*, 283–292. https://doi.org/10.1016/S0959-6526(00)00027-5

Meijide, A., de la Rua, C., Guillaume, T., Röll, A., Hassler, E., Stiegler, C., Tjoa, A., June, T., Corre, M. D., & Veldkamp, E. (2020). Measured greenhouse gas budgets challenge emission savings from palm-oil biodiesel. *Nature Communications*, *11*, 1–11.

Melling, L., Hatano, R., & Goh, K. J. (2005). Soil CO_2 flux from three ecosystems in tropical peatland of Sarawak, Malaysia. *Tellus B: Chemical and Physical Meteorology*, *57*, 1–11. https://doi.org/10.3402/tellusb.v57i1.16772

Miettinen, J., Hooijer, A., Vernimmen, R., Liew, S. C., & Page, S. E. (2017). From carbon sink to carbon source: Extensive peat oxidation in insular Southeast Asia since 1990. *Environmental Research Letters*, *12*. https://doi.org/10.1088/1748-9326/aa5b6f

Miettinen, J., Shi, C., & Liew, S. C. (2016). Land cover distribution in the peatlands of Peninsular Malaysia, Sumatra and Borneo in 2015 with changes since 1990. *Global Ecology and Conservation*, *6*, 67–78. https://doi.org/10.1016/j.gecco.2016.02.004

Moncrieff, J., Clement, R., Finnigan, J., & Meyers, T. (2004). Averaging, detrending, and filtering of eddy covariance time series. In X. Lee, W. Massman, & B. Law (Eds.), *Handbook of micrometeorology: A guide for surface flux measurement and analysis* (pp. 7–31). Dordrecht: Springer Netherlands.

Moncrieff, J. B., Massheder, J., de Bruin, H., Elbers, J., Friborg, T., Heusinkveld, B., Kabat, P., Scott, S., Søgaard, H., & Verhoef, A. (1997). A system to measure surface fluxes of momentum, sensible heat, water vapour and carbon dioxide. *Journal of Hydrology*, *188*, 589–611. https://doi.org/10.1016/S0022-1694(96)03194-0

Moradi, A., Teh, C., Goh, K., Husni, M., & Ishak, C. (2014). Decomposition and nutrient release temporal pattern of oil palm residues. *Annals of Applied Biology*, *164*, 208–219.

Myhre, G., Shindell, D., Pongratz, J., Bréon, F.-M., Collins, W., Fuglestvedt, J., Huang, J., Koch, D., Lamarque, J.-F., Lee, D., Mendoza, B., Nakajima, T., Robock, A., Stephens, G., Takemura, T., & Zhang, H. (2013). Anthropogenic and natural radiative forcing. In T. F. Stocker, D. Qin, G.-K. Plattner, M. Tignor, S. K. Allen, J. Doschung, A. Nauels, Y. Xia, V. Bex, & P. M. Midgley (Eds.), *Climate change 2013: The physical science basis. Contribution of working group I to the fifth assessment report of the Intergovernmental Panel on Climate Change* (pp. 659–740). Cambridge University Press. https://doi.org/10.1017/CBO9781107415324.018

Olson, J. S. (1963). Energy storage and the balance of producers and decomposers in ecological systems. *Ecology*, *44*, 322–331. https://doi.org/10.2307/1932179

Padfield, R., Drew, S., Syayuti, K., Page, S., Evers, S., Campos-Arceiz, A., Kangayatkarasu, N., Sayok, A., Hansen, S., & Schouten, G. (2016). Landscapes in transition: An analysis of sustainable policy initiatives and emerging corporate commitments in the palm oil industry. *Landscape Research*, *41*(7), 744–756. https://doi.org/10.1080/01426397.2016.1173660

Page, S. E., Morrison, R., Malins, C., Hooijer, A., Rieley, J. O., & Jauhiainen, J. (2011). Review of peat surface greenhouse gas emissions from oil palm plantations in Southeast Asia (ICCT White Paper 15). Washington: International Council on Clean Transportation.

Papale, D., Reichstein, M., Aubinet, M., Canfora, E., Bernhofer, C., Kutsch, W., Longdoz, B., Rambal, S., Valentini, R., Vesala, T., & Yakir, D. (2006). Towards a standardized processing of Net Ecosystem Exchange measured with eddy covariance technique: Algorithms and uncertainty estimation. *Biogeosciences*, *3*, 571–583. https://doi.org/10.5194/bg-3-571-2006

Pranantо, J. A., Minasny, B., Comeau, L. P., Rudiyanto, R., & Grace, P. (2020). Drainage increases CO_2 and N_2O emissions from tropical peat soils. *Global Change Biology*, *26*, 4583–4600. https://doi.org/10.1111/gcb.15147

Qaim, M., Sibhatu, K. T., Siregar, H., & Grass, I. (2020). Environmental, economic, and social consequences of the oil palm boom. *Annual Review of Resource Economics*, *12*, 321–344. https://doi.org/10.1146/annurev-resource-110119-024922

R Core Team (2018). *R: A language and environment for statistical computing*. Vienna, Austria: R Foundation for Statistical Computing. https://www.R-project.org/

Reichstein, M., Falge, E., Baldocchi, D., Papale, D., Aubinet, M., Berbigier, P., Bernhofer, C., Buchmann, N., Gilmanov, T., & Granier, A. (2005). On the separation of net ecosystem exchange into assimilation and ecosystem respiration: Review and improved algorithm. *Global Change Biology*, *11*, 1424–1439. https://doi.org/10.1111/j.1365-2486.2005.001002.x

Schmidt, J. H. (2015). Life cycle assessment of five vegetable oils. *Journal of Cleaner Production*, *87*, 130–138. https://doi.org/10.1016/j.jclepro.2014.10.011

Stiegler, C., Meijide, A., Fan, Y., Ashween Ali, A., June, T., & Knohl, A. (2019). El Niño-Southern Oscillation (ENSO) event reduces CO_2 uptake of an Indonesian oil palm plantation. *Biogeosciences*, *16*, 2873–2890. https://doi.org/10.5194/bg-16-2873-2019

Stineman, R. W. (1980). A consistently well-behaved method of interpolation. *Creative Computing*, *6*, 54–57.

Swails, E., Jaye, D., Verchot, L., Hergoualc'h, K., Schirrmann, M., Borchard, N., Wahyuni, N., & Lawrence, D. (2017). Will CO_2 emissions from drained tropical peatlands decline over time? Links between soil organic matter quality, nutrients, and C mineralization rates. *Ecosystems*, *21*, 868–885. https://doi.org/10.1007/s10021-017-0190-4

Tang, A. C., Melling, L., Stoy, P. C., Musin, K. K., Aeries, E. B., Waili, J. W., Shimizu, M., Poulter, B., & Hirata, R. (2020). A Bornean peat swamp forest is a net source of carbon dioxide to the atmosphere. *Global Change Biology*, *26*(12), 6931–6944. https://doi.org/10.1111/gcb.15332

Vickers, D., & Mahrt, L. (1997). Quality control and flux sampling problems for tower and aircraft data. *Journal of Atmospheric and Oceanic Technology*, *14*, 512–526.

Wijedasa, L. S., Jauhiainen, J., Kononen, M., Lampela, M., Vasander, H., Leblanc, M. C., Evers, S., Smith, T. E., Yule, C. M., Varkkey, H., & Lupascu, M. (2017). Denial of long-term issues with agriculture on tropical peatlands will have devastating consequences. *Global Change Biology*, *23*, 977–982. https://doi.org/10.1111/gcb.13516

Wijedasa, L. S., Sloan, S., Page, S. E., Clements, G. R., Lupascu, M., & Evans, T. A. (2018). Carbon emissions from South-East Asian peatlands will increase despite emission-reduction schemes. *Global Change Biology*, *24*, 4598–4613. https://doi.org/10.1111/gcb.14340

Wilczak, J. M., Oncley, S. P., & Stage, S. A. (2001). Sonic anemometer tilt correction algorithms. *Boundary-Layer Meteorology*, *99*, 127–150.

Wilson, K., Goldstein, A., Falge, E., Aubinet, M., Baldocchi, D., Berbigier, P., Bernhofer, C., Ceulemans, R., Dolman, H., & Field, C. (2002). Energy balance closure at FLUXNET sites. *Agricultural and Forest Meteorology*, *113*, 223–243. https://doi.org/10.1016/S0168-1923(02)00109-0

Wösten, J., Ismail, A., & van Wijk, A. (1997). Peat subsidence and its practical implications: A case study in Malaysia. *Geoderma*, *78*, 25–36. https://doi.org/10.1016/S0016-7061(97)00013-X

Wutzler, T., Lucas-Moffat, A., Migliavacca, M., Knauer, J., Sickel, K., Šigut, L., Menzer, O., & Reichstein, M. (2018). Basic and extensible post-processing of eddy covariance flux data with REddyProc. *Biogeosciences*, *15*, 5015–5030. https://doi.org/10.5194/bg-2018-56

Xu, J., Morris, P. J., Liu, J., & Holden, J. (2018). PEATMAP: Refining estimates of global peatland distribution based on a meta-analysis. *Catena*, *160*, 134–140. https://doi.org/10.1016/j.catena.2017.09.010

SUPPORTING INFORMATION

Additional supporting information may be found online in the Supporting Information section.

How to cite this article: McCalmont J, Kho LK, Teh YA, et al. Short- and long-term carbon emissions from oil palm plantations converted from logged tropical peat swamp forest. *Glob Change Biol*. 2021;27:2361–2376. https://doi.org/10.1111/gcb.15544